



Synthesis Theory and Optimum Design of Four-bar Linkage with Given Angle Parameters

Lairong Yin¹, Long Huang¹, Juan Huang², Peng Xu³, Xuejun Peng¹, and Peng Zhang^{1,4}

¹School of Automotive and Mechanical Engineering, Changsha University of Science and Technology, Changsha, 410114, China

²College of Engineering, Hunan Agriculture University, Changsha, 410012, China

³Hunan Changzhong Machinery co.Ltd, Changsha, 410014, China

⁴Hunan Provincial Key Laboratory of Intelligent Manufacturing Technology for High-performance Mechanical Equipment, Changsha University of Science and Technology, Changsha 410114, China

Correspondence: Long Huang (huanglongin@foxmail.com) and Juan Huang (35488869@qq.com)

Received: 23 June 2019 – Revised: 9 October 2019 – Accepted: 26 October 2019 – Published: 15 November 2019

Abstract. In this paper, a synthesis method is proposed for the 5-point-contact four-bar linkage that approximates a straight line with given angle parameters. The given parameters were the angles and the location of the Ball point. Synthesis equations were derived for a general Ball–Burmester point case, the Ball–Burmester point at an inflection pole, and the Ball point that coincided with two Burmester points, resulting in three respective groups of bar linkages. Next, taking Ball–Burmester point as the coupler point, two out of the three bar-linkage combinations were used to generate three four-bar mechanisms that shared the same portion of a rectilinear trajectory. Computation examples were presented, and nine cognate straight-line mechanisms were obtained based on the Roberts–Chebyshev theory. Considering that the given parameters were angles which was arbitrarily chosen, with the other two serving as the horizontal and vertical axes, so the solution region graphs of the solutions for three mechanism configurations were plotted. Based on these graphs, the distribution of the mechanism attributes was obtained with high efficiency. By imposing constraints, the optimum mechanism solution was straightforwardly identified by the designers. For the angular parameters prescribed in this paper, the solutions for three straight-line mechanism configurations were obtained, along with nine cognate straight-line mechanisms that shared the same portion of the rectilinear trajectory. All the fixed pivot installation locations and motion performances differed, thus providing multiple solutions to the trajectory of the synthesis of mechanisms.

1 Introduction

The synthesis and optimization of mechanisms is a key technology in modern equipment innovations such as those in ship building, power locomotives and construction machinery, to name a few. As modern machinery continues to move toward greater automation and intelligence, due to the advantages of reliable support, strong bearing capacity, and easy processing, linkage mechanisms play an increasingly important role. As such, research on new synthesis methods and application technologies is attracting the attention of more and more specialists in the field of mechanics (Han, 1993; McCarthy, 2000). Brake et al. discussed the Complete Solution of Alt–Burmester Synthesis Problems for Four-Bar

Linkages (Brake et al., 2016). Bulatović et al. (2016) developed a variable controlled deviations method and modified Krill Herd (MKH) algorithm to synthesize four-bar linkages for accomplishing approximately rectilinear motion (Bulatović and Dordević, 2009; Bulatović et al., 2016). Singh et al. (2017) used nature inspired optimization algorithms to reduce the computation and get the crank-rocker mechanisms without defects (Singh et al., 2017). Slesongsoma and Bureerat (2017) proposed a variant of teaching-learning-based-optimization for four-bar linkage path generation, which was significantly superior to its original version (Slesongsoma and Bureerat, 2017). Deshpande and Purwar (2017) proposed a novel algorithm for optimal approximate synthesis of

Burmester problem with no exact solutions (Deshpande and Purwar, 2017). Wang et al. (2019) developed a program package based on Matlab for the synthesis calculation of planar 4R linkage based on the theory of planar analytic geometry (Wang et al., 2019). Ramanpreet et al. proposed a refinement scheme for the optimal syntheses of the planar crank-rocker linkage free from all defects, which is used in human knee exoskeleton (Singh et al., 2017). Bulatović and Dordević (2009) proposed the variable controlled deviations method to synthesize planar four-bar mechanisms for accomplishing approximately rectilinear motion. Slesongsoma and Bureerat (2017) introduced a variant of teaching-learning-based-optimization, which was significantly superior to its original version. Singh et al. (2017) proposed an optimization algorithm based on TLBO, which could reduce the computation and get the crank-rocker mechanisms without defects. A straight-line motion mechanism refers to one whose points occupy a portion of a trajectory that is approximately or precisely rectilinear (Vidosic and Tesar, 1967; Dijksman, 1976; Yu et al., 2013; Yin et al., 2019). Numerous researchers have worked on the synthesis theory and developed optimization methods for such mechanisms (Han et al., 2009; Han and Cao, 2018; Yang et al., 2011; Cui and Han, 2016). Chen et al. (2013, 2016) focused on the design and analysis of compliant Sarrus straight-line mechanisms, and developed several straight-line mechanisms with special performance (Chen et al., 2013, 2016).

In the practical application of hinged four-bar straight-line mechanisms, the designers usually have specific requirements regarding the installation locations, dimensions, and performance of the fixed pivots, and there can be an infinite number of mechanisms that might satisfy these requirements. Therefore, selection of the optimum mechanism solution that best satisfies the practical engineering conditions is a difficult problem that has puzzled designers.

In this paper, a synthesis method is proposed for the 5-point-contact four-bar linkage that approximates a straight line with given angle parameters. The given parameters were the angles and the location of the Ball point. Synthesis equations were derived for a general Ball–Burmester point case, the Ball–Burmester point at an inflection pole, and the Ball point that coincided with two Burmester points, resulting in three respective groups of bar linkages. Next, taking Ball–Burmester point as the coupler point, two out of the three bar-linkage combinations were used to generate three four-bar mechanisms that shared the same portion of a rectilinear trajectory. Computation examples were presented, and nine cognate straight-line mechanisms were obtained based on the Roberts-Chebyshev theory. Considering that the given parameters were angles which was arbitrarily chosen, with the other two serving as the horizontal and vertical axes, so the solution region graphs of the solutions for three mechanism configurations were plotted. Based on these graphs, the distribution of the mechanism attributes was obtained with high efficiency. By imposing constraints, such as the mech-

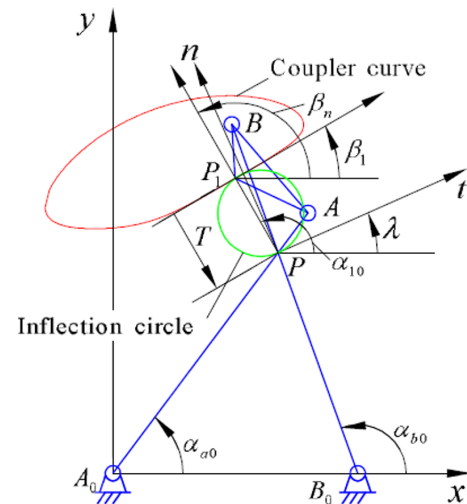


Figure 1. Definitions of various parameters (Yin et al., 2019).

anism type, the ratio of the longest to the shortest link, the minimum transmission angle, and the length of approximate straight-line, the optimum mechanism solution was straightforwardly identified by the designers. For the angular parameters prescribed in this paper, the solutions for three straight-line mechanism configurations were obtained, along with nine cognate straight-line mechanisms that shared the same portion of the rectilinear trajectory. All the fixed pivot installation locations and motion performances differed, thus providing multiple solutions to the trajectory of the synthesis of mechanisms. The designers obtained intuitively mechanism properties involved and avoided aimlessness in traditional optimum design methods mentioned in the references. The optimal mechanism with expected parameters could be selected more precisely and rapidly as the synthesizing process was visible and automatic.

2 Synthesis equations

Based on theories of kinematic geometry for points with infinite proximity, it is well known that the motion of a rigid body can be described as the pure rolling of its instantaneous center line on its fixed centrode. The curvature relationship of trajectory of any point on a moving system is determined in terms of Euler-Savary equation. The Euler-Savary equation is $\frac{1}{PA} - \frac{1}{PA_0} = \frac{1}{D \sin \alpha}$ or $\frac{1}{r} - \frac{1}{r+\rho} = \frac{1}{D \sin \alpha}$ or $\rho = \frac{r}{D \sin \alpha - r}$; Where, D is defined as the diameter of inflexion circle; PA and PA_0 are vectors, as shown in Fig. 1. The relevant fundamental theories and parameter definitions are described in detail in Yin et al. (2012) and Yin and Han (2011) and are not repeated here. Taking the instantaneous center pole P as the coordinate origin, we draw a unit circle along the positive y axis and tangent x axis at the origin. The angles between PA , PB , PC , PP_1 and the positive x axis are α_a , α_b , α_c , and α_1 , respectively, as illustrated in Fig. 1.

Taking the second-order derivative of the Euler-Savary equation $\rho_m = \frac{r}{D \sin \alpha - r}$, we obtain:

$$\tan^4 \alpha + \frac{N(M-2)}{M} \tan^3 \alpha + \left(\frac{dN}{d\sigma} - 1 \right) \tan^2 \alpha + \frac{N^2 \frac{dM}{d\sigma} - 3NM}{M^2} \tan \alpha + \frac{N^2(1-M)}{M^2} = 0, \quad (1)$$

where M and N are auxiliary variables: $\frac{1}{M} = \frac{1}{3} \left[\frac{1}{D} + \frac{1}{\rho_m} \right]$, $\frac{1}{N} = -\frac{1}{3D} \frac{dD}{d\sigma}$.

Equation (1) is a quartic equation for a single variable and it has four real roots at most. These four roots give the α_i of Burmester points' polar coordinates by employing Mueller's concepts on the highest attainable order of straight lines (Kwun-Lon Ting, 1991). Movable joints A , B , and C correspond to the three roots of α_a , α_b , and α_c , respectively. The coupler point P_1 corresponds to one root of α_1 .

From the relationship between the roots and coefficients of a quadratic equation, one obtains:

$$\tan^2 \alpha + \left[\tan \alpha_a + \tan \alpha_b + \frac{N(M-2)}{M} \right] \tan \alpha + \frac{N^2(1-M)}{M^2 \tan \alpha_a \tan \alpha_b} = 0, \quad (2)$$

where $\tan \alpha_1$ and $\tan \alpha_c$ are the two roots of the quadratic equation.

To simplify the calculation, in this paper, the diameter of the inflection circle is taken as $D = 1$. The final solution can be multiplied by the diameter of the practical inflection circle. Now, we solve for the joint coordinates of the four-bar mechanisms under various given conditions.

2.1 General case of Ball–Burmester point

For a general case of a Ball–Burmester point, the given parameters are the angles α_a , α_b , and α_1 . From Eq. (2), the value of α_c can be computed as follows:

$$\alpha_c = \tan^{-1} \left(-\frac{2 \tan \alpha_1 + V}{U + 1} \right), \quad (3)$$

where $U = \tan \alpha_a \tan \alpha_b$ and $V = \tan \alpha_a + \tan \alpha_b$.

By definition, one obtains the following:

$$PP_1 = D \sin \alpha_1. \quad (4)$$

Therefore, the coordinates of the Ball–Burmester point can be obtained as follows:

$$\begin{cases} P_{1x} = PP_1 \times \cos \alpha_1 \\ P_{1y} = PP_1 \times \sin \alpha_1 \end{cases} \quad (5)$$

PA , PB and PC can be computed from the following respective equations:

$$PA = \frac{[(3U + 1) \tan \alpha_1 + UV] \sin \alpha_a}{(U + 1) \tan \alpha_a + U(2 \tan \alpha_1 + V)}, \quad (6)$$

$$PB = \frac{[(3U + 1) \tan \alpha_1 + UV] \sin \alpha_b}{(U + 1) \tan \alpha_b + U(2 \tan \alpha_1 + V)}, \quad (7)$$

$$PC = \frac{[(3U + 1) \tan \alpha_1 + UV] \sin \alpha_c}{(U - 1)(2 \tan \alpha_1 + V)}. \quad (8)$$

From the geometric relationships, the coordinates of movable joints A , B , and C are as follows:

$$\begin{cases} A_x = PA \times \cos \alpha_a \\ A_y = PA \times \sin \alpha_a \end{cases}, \quad (9)$$

$$\begin{cases} B_x = PB \times \cos \alpha_b \\ B_y = PB \times \sin \alpha_b \end{cases}, \quad (10)$$

$$\begin{cases} C_x = PC \times \cos \alpha_c \\ C_y = PC \times \sin \alpha_c \end{cases}. \quad (11)$$

From the equations:

$$\begin{cases} PA_0 = -\frac{PA \cdot D \sin \alpha_a}{PA - D \sin \alpha_a} \\ PB_0 = -\frac{PB \cdot D \sin \alpha_b}{PB - D \sin \alpha_b} \\ PC_0 = -\frac{PC \sin \alpha_c}{PC - \sin \alpha_c} \end{cases}, \quad (12)$$

PA_0 , PB_0 , PC_0 can be solved. In turn, the coordinates of fixed joints A_0 , B_0 , C_0 can be obtained as follows:

$$\begin{cases} A_{0x} = PA_0 \times \cos \alpha_a \\ A_{0y} = PA_0 \times \sin \alpha_a \end{cases}, \quad (13)$$

$$\begin{cases} B_{0x} = PB_0 \times \cos \alpha_b \\ B_{0y} = PB_0 \times \sin \alpha_b \end{cases}, \quad (14)$$

$$\begin{cases} C_{0x} = PC_0 \times \cos \alpha_c \\ C_{0y} = PC_0 \times \sin \alpha_c \end{cases}. \quad (15)$$

When the coordinates of all the joints are available, the three groups of bar linkages AA_0 , BB_0 , CC_0 can be obtained. Taking Ball–Burmester point P_1 as the coupler point, two out of the three bar linkage combinations can be used to generate three four-bar straight-line mechanisms.

2.2 Ball–Burmester point lying on the inflection pole

When the Ball–Burmester point is on inflection-circle pole, the given parameters are angle α_a and parameter D' , where D' is the diameter when the trajectory of the circle center degenerates into a circle. Coupler point P_1 is the inflection pole. The remaining parameters of the mechanism are computed as follows:

$$PA_0 = D' \sin \alpha_a, \quad (16)$$

$$PA = \frac{PA_0}{D' + 1}, \quad (17)$$

$$\alpha_b = \tan^{-1} \left(-\frac{D' + 1}{D' + 3} \cdot \frac{1}{\tan \alpha_a} \right), \quad (18)$$

$$PB_0 = D' \sin \alpha_b, \quad (19)$$

$$PB = \frac{PB_0}{D' + 1}. \quad (20)$$

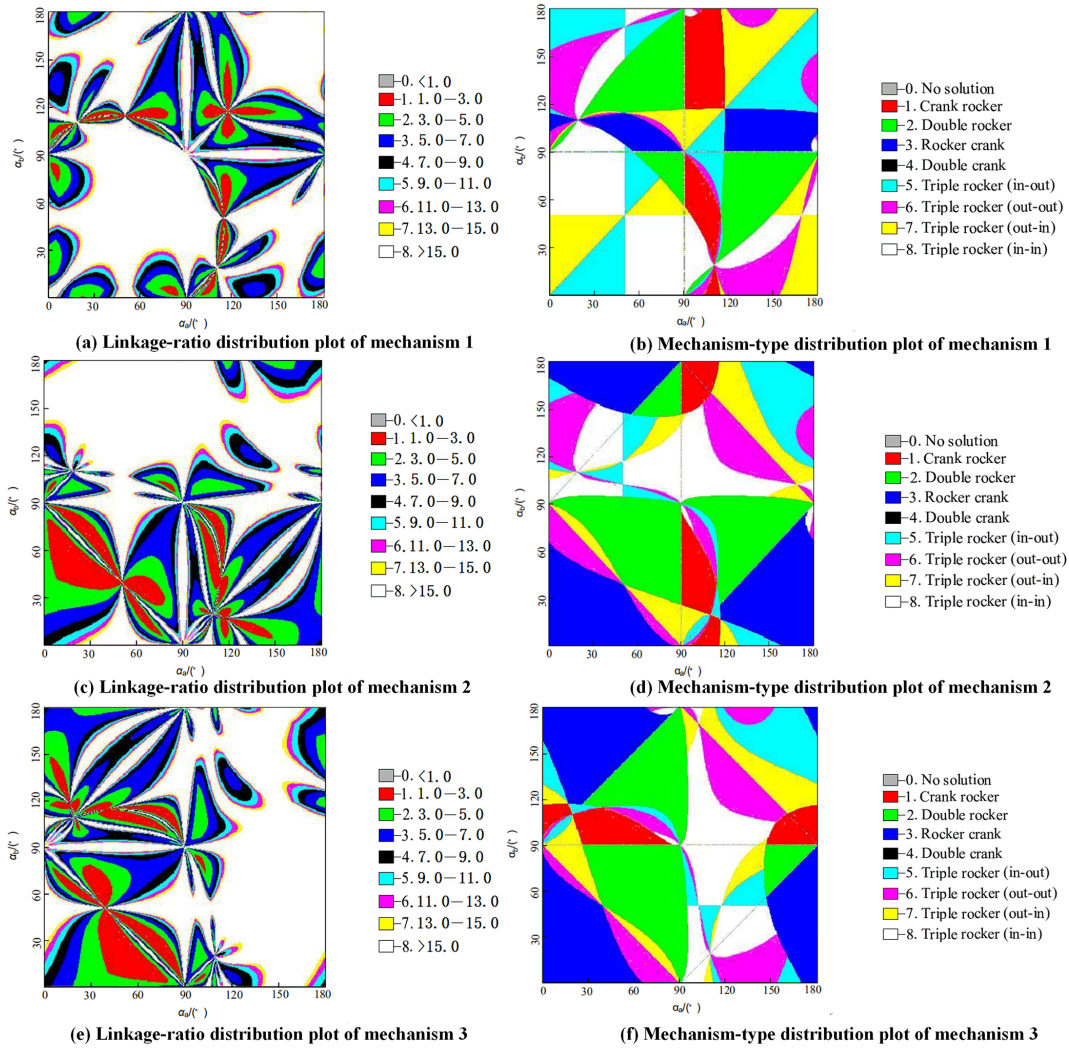


Figure 2. Linkage ratio distribution and Mechanism type distribution plots.

Table 1. Parameters of mechanisms.

Mechanisms	The length of links					l_{sum}	$\frac{l_{max}}{l_{min}}$	Type of mechanisms
	A_0A	AB	B_0B_0	A_0B_0	AP_1			
M_{1-1}	258.18	89.66	85.56	100.56	73.10	533.96	3.01	5-three rocker
M_{1-2}	258.18	185.08	31.14	106.23	73.10	580.63	8.29	3-rocker-crank
M_{1-3}	85.56	95.42	31.14	48.44	82.63	260.56	3.06	3-rocker-crank
M_{2-1}	45.60	65.39	114	196.16	94.66	421.15	4.30	8-three rocker
M_{2-2}	45.60	27.48	8.33	65.04	94.66	146.45	7.81	3-rocker-crank
M_{2-3}	114	37.91	8.33	143.54	59.18	303.78	17.23	3-rocker-crank
M_3	8.48	23.39	42.48	56.61	59.90	130.96	6.68	1-crank-rocker

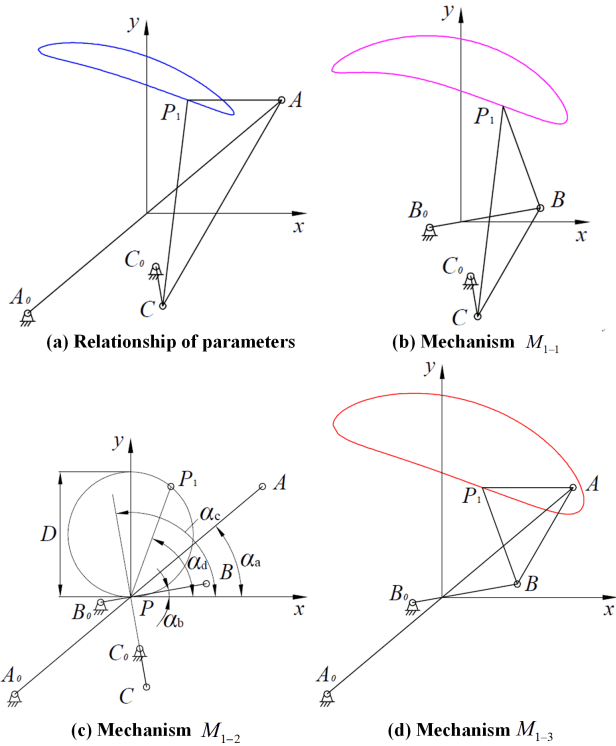


Figure 3. Mechanism plots.

In this situation, $\alpha_c = 90^\circ$.

$$PC = \frac{D'}{2D' + 4} \tag{21}$$

$$PC_0 = \frac{D'}{D' + 4} \tag{22}$$

After computing the above parameters, similar to Eq. (1), the coordinates of movable joints A , B , and C and fixed joints A_0 , B_0 , and C_0 can be solved to obtain three four-bar straight-line mechanism.

2.3 Ball point coinciding with two Burmester points

When two Burmester points coincide with the Ball point, the given parameters are angles α_a and α_b . Every group of given parameters can only generate one four-bar straight-line mechanism. The remaining parameters of this mechanism are computed as follows:

$$\alpha_1 = \tan^{-1} \left(-\frac{V}{U + 3} \right), \tag{23}$$

where $U = \tan \alpha_a \tan \alpha_b$ and $V = \tan \alpha_a + \tan \alpha_b$.

By substituting Eq. (23) into $PP_1 = D \sin \alpha_1$, PP_1 can be solved.

$$PA = \frac{V(U - 1) \sin \alpha_a}{(U + 3) \tan \alpha_a + U \cdot V} \tag{24}$$

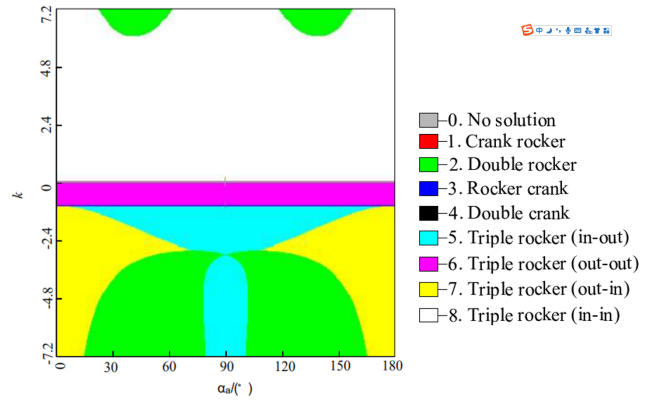


Figure 4. Mechanism type distribution plot.

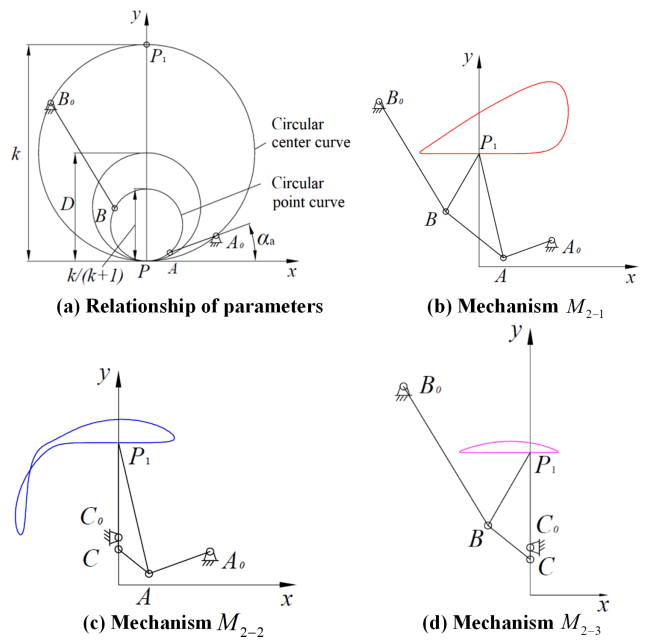


Figure 5. Mechanism plots.

$$PB = \frac{V(U - 1) \sin \alpha_b}{(U + 3) \tan \alpha_b + U \cdot V} \tag{25}$$

By substituting Eqs. (24) and (25) into the following two equations:

$$\begin{cases} PA_0 = -\frac{PA \cdot D \sin \alpha_a}{PA - D \sin \alpha_a} \\ PB_0 = -\frac{PB \cdot D \sin \alpha_b}{PB - D \sin \alpha_b} \end{cases}, \tag{26}$$

PA_0 and PB_0 can be obtained. After the above parameters have been computed, the coordinates of movable joints A , B , and C and fixed joints A_0 , B_0 , and C_0 can be solved to obtain one four-bar straight-line mechanism.

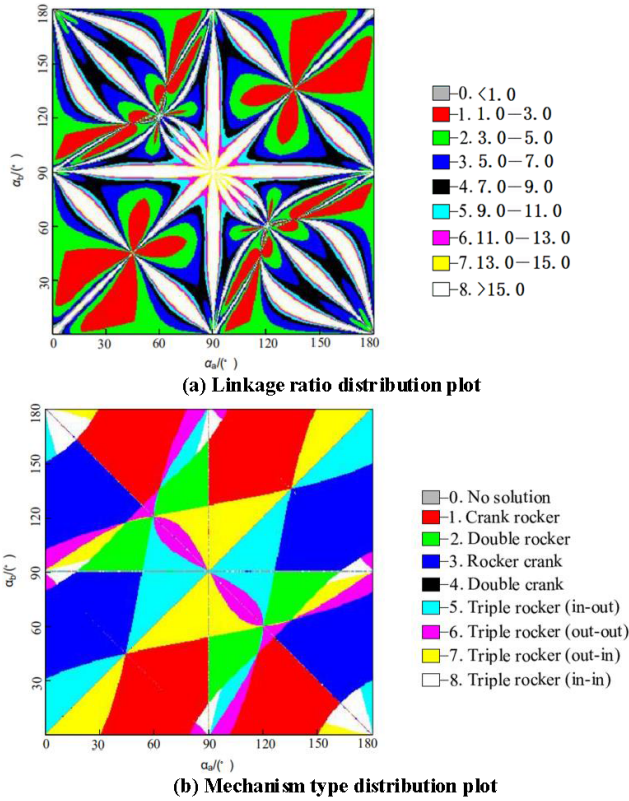


Figure 6. Linkage-ratio distribution and mechanism-type distribution plot.

3 Solution region analysis and synthesis examples

Now, we adopted the mechanism solution region method, taking the inflection circle diameter $D=1$ and the mechanism-type distribution plot as an example to draw the mechanism solution region graphs for all three conditions.

3.1 General Case of the Ball–Burmester Point

Without losing generality, let $\alpha_1 = 70^\circ$, take α_a and α_b as the horizontal and vertical axes, respectively, and let α_a and α_b take continuous values from 0 to 180° to obtain solution region graphs for three mechanism configurations, as illustrated in Fig. 2 (Barker, 1985).

By arbitrarily choosing $\alpha_a = 40^\circ$ and $\alpha_b = 10^\circ$ in Fig. 2, Fig. 3b shows the obtained mechanism, and Fig. 3c and d show the two corresponding mechanism solutions. Table 1 lists the mechanism parameters.

3.2 Ball–Burmester point lying on the inflection pole

Take α_a as the horizontal axis and the diameter of the degenerated circular center curve D' as the vertical axis and let parameter D' take continuous values from -7.2 to 7.2 and angle α_a take continuous values from 0 to 180° , then the solution region graphs of the three mechanism configurations

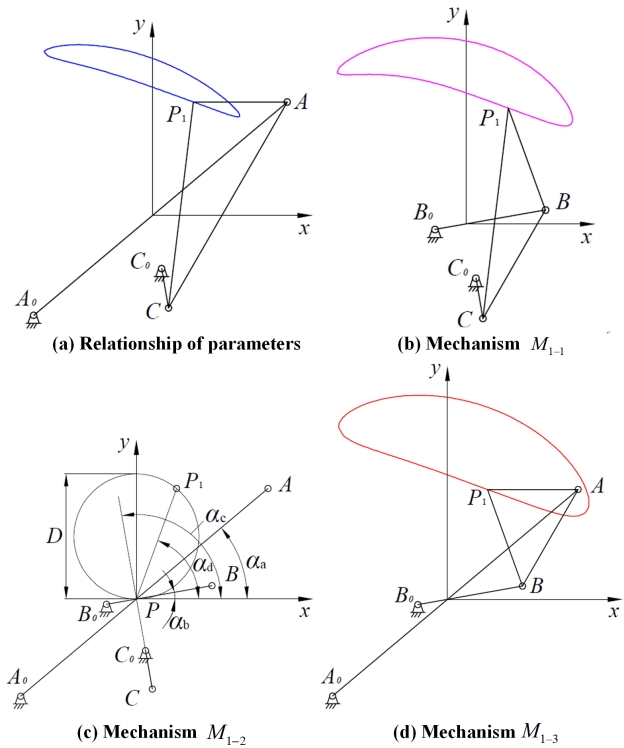


Figure 7. Mechanism M_3 .

can be obtained. Figure 4 shows the mechanism-type distribution graph for the first configuration $A_0AB_0BP_1$.

By arbitrarily choosing $\alpha_a = 20^\circ$ and $D' = 2$ in Fig. 4, Fig. 5b shows the obtained mechanism, and Fig. 5c and d show the other two mechanisms. Table 1 lists the mechanism parameters.

3.3 Ball point coinciding with two Burmester points

Similar to Eq. (1), by taking α_a as the horizontal axis and α_b as the vertical axis, we obtained the mechanism type of the single mechanism configuration $A_0AB_0BP_1$ and its linkage-ratio distribution plot, as shown in Fig. 6. By arbitrarily choosing $\alpha_a = 100^\circ$ and $\alpha_b = 150^\circ$ in Fig. 6, Fig. 7 shows the obtained mechanism. Table 1 shows the mechanism parameters.

4 Conclusion

Using the synthesis method proposed in this paper combined with the cognate mechanism theory, nine different four-bar mechanisms with identical rectilinear trajectory sections were obtained that have different frame locations and performances for the designer to choose. Given that the known parameters were angular, this method was used to obtain the solution region graphs of three mechanism solutions. Based on these solution region graphs, the distribution of the attributes of the mechanism solutions was obtained with high effi-

ciency, and the optimum solution was extracted in a straightforward manner. The optimum design mentioned in the paper was to choose optimum mechanism from the infinite number of mechanism solutions. By imposing constraints, such as the mechanism type, the ratio of the longest to the shortest link, the minimum transmission angle, and the length of approximate straight-line, the optimum mechanism solution was straightforwardly identified by the designers. The design data have been obtained and converted into a series of design graphs by the computer program which can be used to synthesize easily four-bar linkages yielding desired straight-line outputs of predetermined position. The method proposed in this paper represents a new approach to the synthesis of classic straight-line mechanisms and has high value in practical applications.

Data availability. All the data used in this manuscript can be obtained on request from the corresponding author.

Author contributions. LY proposed the idea and methodology; LH derived the equations; JH, PX, XP and PZ developed the software.

Competing interests. The authors declare that they have no conflict of interest.

Acknowledgements. This work has been financially supported by the National Natural Science Foundation of China (Nos. 51705034 and 51805047), the Natural Science Foundation of Hunan province (Nos. 2018JJ3548 and 2019JJ50664), and Innovation Platform Foundation of Key Laboratory of Safety Design and Reliability Technology for Engineering Vehicle of Hunan Provincial Department of Education (17K003).

Financial support. This research has been supported by the National Natural Science Foundation of China (grant nos. 51705034, 51805047), the Natural Science Foundation of Hunan Province (grant nos. 2018JJ3548, 2019JJ50664), and the Innovation Platform Foundation of Key Laboratory of Safety Design and Reliability Technology for Engineering Vehicle of Hunan Provincial Department of Education (grant no. 17K003).

Review statement. This paper was edited by Guimin Chen and reviewed by three anonymous referees.

References

Barker, C. A.: A complete classification of planar four-bar linkages, *Mech. Mach. Theory*, 20, 535–554, [https://doi.org/10.1016/0094-114X\(85\)90071-0](https://doi.org/10.1016/0094-114X(85)90071-0), 1985.

- Brake, D. A., Hauenstein, J. D., Murray, A. P., Myszka D. H., and Wampler, C. W.: The Complete Solution of Alt–Burmester Synthesis Problems for Four-Bar Linkages, *J. Mech. Robot.*, 8, 041018, <https://doi.org/10.1115/1.4033251>, 2016.
- Bulatović, R. R. and Dordević, S. R.: On the optimum synthesis of a four-bar linkage using differential evolution and method of variable controlled deviations, *Mech. Mach. Theory*, 44, 235–246, 2009.
- Bulatović, R. R., Miodragović, G., and Bošković, M. S.: Modified Krill Herd (MKH) algorithm and its application in dimensional synthesis of a four-bar linkage, *Mech. Mach. Theory*, 95, 1–21, 2016.
- Chen, G. M., Zhang, S. Y., and Li, G. Multistable Behaviors of Compliant Sarrus Mechanisms, *J. Mech. Robotics*, 5, 021005, <https://doi.org/10.1115/1.4023557>, 2013.
- Chen, G. M., Chang, H. Y., and Li, G.: Design of Constant-Force Compliant Sarrus Mechanism Considering Stiffness Nonlinearity of Compliant Joints, in: *Advances in Reconfigurable Mechanisms and Robots II. Mechanisms and Machine Science*, edited by: Ding, X., Kong, X., and Dai, J., Springer, Switzerland, 36, https://doi.org/10.1007/978-3-319-23327-7_10, 2016.
- Cui, G. Z. and Han, J. Y.: The solution region-based synthesis methodology for a 1-DOF eight-bar linkage, *Mech. Mach. Theory*, 98, 231–241, <https://doi.org/10.1016/j.mechmachtheory.2015.12.011>, 2016.
- Deshpande, S. and Purwar, A.: A Task-Driven Approach to Optimal Synthesis of Planar Four-Bar Linkages for Extended Burmester Problem, *ASME J. Mech. Robotics*, 9, 061005, <https://doi.org/10.1115/1.4037801>, 2017.
- Dijkman, E. A.: *Motion geometry of mechanisms*, Cambridge University Press, Cambridge, UK, 1976.
- Han, J. Y.: Ein Beitrag zur rechnerunterstützten Masssynthese ebener Gelenkgetriebe fuer angenaeherte Geradfuehrungen durch vier bzw. fuenf unendlich benachbarte Punkte, Dissertation Universitaet der Bundeswehr, Universitaet der Bundeswehr, Hamburg, Germany, 1993.
- Han, J. Y. and Cao, Y.: Analytical synthesis methodology of RCCC linkages for the specified four poses, *Mech. Mach. Theory*, 133, 531–540, <https://doi.org/10.1016/j.mechmachtheory.2018.12.005>, 2018.
- Han, J. Y., Qian, W. X., and Zhao, H. S.: Study on synthesis method of λ -formed 4-bar linkages approximating a straight line, *Mech. Mach. Theory*, 44, 57–65, <https://doi.org/10.1016/j.mechmachtheory.2008.02.011>, 2009.
- Kwun-Lon Ting, S. C. W.: Fourth and fifth order double Burmester points and the highest attainable order of straight lines, *ASME J. Mech. Design*, 113, 213–219, <https://doi.org/10.1115/1.2912771>, 1991.
- McCarthy, J. M.: *Geometric Design of Linkages*, Springer-Verlag, New York, 2000.
- Singh, R., Chaudhary, H., and Singh, A. K.: Defect-free optimal synthesis of crank-rocker linkage using nature-inspired optimization algorithms, *Mech. Mach. Theory*, 116, 105–122, <https://doi.org/10.1016/j.mechmachtheory.2017.05.018>, 2017.
- Sleesongsom, S. and Bureerat, S.: Four-bar linkage path generation through self-adaptive population size teaching learning based optimization, *Knowledge-Based Systems*, 135, 180–191, 2017.
- Vidosic, J. P. and Tesar, D.: Selections of four-bar mechanisms having required approximate straight-line outputs, part III, the

- Ball-Double Burmester point Linkage, *J. Mechanisms*, 2, 61–78, [https://doi.org/10.1016/0022-2569\(67\)90055-9](https://doi.org/10.1016/0022-2569(67)90055-9), 1967.
- Wang, G., Zhang, H., Li, X., Wang, J., Zhang, X., and Fan, G.: Computer-aided synthesis of spherical and planar 4R linkages for four specified orientations, *Mech. Sci.*, 10, 309–320, <https://doi.org/10.5194/ms-10-309-2019>, 2019.
- Yang, T., Han, J. Y., and Yin, L. R.: A unified synthesis method based on solution regions for four-position finitely separated and mixed “Point-Order” positions, *Mech. Mach. Theory*, 46, 1719–1731, <https://doi.org/10.1016/j.mechmachtheory.2011.06.008>, 2011.
- Yin, L., Huang, L., Huang, J., Tian, L., and Li, F.: Solution-region-based synthesis approach for selecting optimal four-bar linkages with the Ball–Burmester point, *Mech. Sci.*, 10, 25–33, <https://doi.org/10.5194/ms-10-25-2019>, 2019.
- Yin, L. R. and Han, J. Y.: Solution region analysis and synthesis method of straight-line mechanism under special configuration, *Transactions of the Chinese Society of Agricultural Machinery*, 42, 190–194, <https://doi.org/10.6041/j.issn.1000-1298.2012.10.036>, 2011.
- Yin, L. R., Han, J. Y., and Mao, C.: Synthesis method based on solution regions for planar four-bar straight-line linkages, *J. Mech. Sci. Technol.*, 26, 3159–3167, <https://doi.org/10.1007/s12206-012-0826-4>, 2012.
- Yu, H. Y., Zhao, Y. W., and Wang, Z. X.: Study on numerical comparison method of four-bar straight-line guidance mechanism, *Journal of Harbin Institute of Technology*, 20, 63–72, <https://doi.org/10.11916/j.issn.1005-9113.2013.04.011>, 2013.